Analysis of Ki67 Density Maps Reveals Variation of Spatial Proliferation Patterns in Different Canine Neoplasms

Analysis of Ki67 density maps reveals variation of spatial proliferation patterns in different canine neoplasms

Running title: spatial proliferation in canine neoplasms

Brigandì Elena[1], Bacci Barbara[1], Brunetti Barbara[1], Rigillo Antonella[2], Roccabianca Paola[3], Bellini Giorgia[1], Chiappelli Chiara[1], Avallone Giancarlo[1]

[1] Department of Veterinary Medical sciences (DIMEVET), University of Bologna, via Tolara di Sopra 50, Ozzano dell'Emilia, Italy

[2]i-Vet, Flero (BS), Italy (AR)

[3]Department of Veterinary Medicine and Animal Sciences, University of Milan, Lodi, Italy (PR)

Corresponding Author:

Giancarlo Avallone

email: giancarlo.avallone@unibo.it

Tel: +39 0512097960

Address: Department of Veterinary Medical Sciences (DIMEVET), University of Bologna, Via Tolara di Sopra 50, 40064 Ozzano dell'Emilia (BO), Italy

Disclaimers: none

Source(s) of support: none

Word count: 2644

Number of figures and tables: 3

Conflict of interest declaration: none

Cell line validation: no cell lines have been used

Ethic statement: there were no animal subject

Data availability statement: data will be available upon request to the corresponding author

Abstract

Mitotic count (MC) is a well-established prognostic factor in many canine malignancies. While standardization efforts have improved inter-pathologist agreement regarding the morphology of mitotic figures and the size of the counting area, the selection of the tumor region for MC assessment remains to be standardized. This study aimed to evaluate the spatial distribution of the most proliferative areas in selected canine tumor types, using Ki67 immunohistochemistry, to identify optimal candidate regions for MC assessment. Tumor types analyzed included melanomas, cutaneous mast cell tumors (cMCT), canine mammary carcinomas (CMC), and soft tissue sarcomas (STS). Using image analysis, Ki67 density maps were generated from digital slides and classified according to their distribution pattern (focal/multifocal or diffuse) and location within the tumor (central, peripheral, or scattered). A total of 202 cases were included: 43 melanomas, 30 cMCTs, 42 CMCs, and 87 cSTSs. The vast majority of tumors (92.6%) exhibited a multifocal hotspot distribution. Peripheral hotspot localization was predominant in 55% of cases, particularly in cMCTs (73.3%) and melanomas (76.7%). In contrast, cSTSs more frequently showed a scattered hotspot pattern (60.9%) ($\chi^2 = 41.9$; $p < 0.001$). CMCs had a higher proportion of centrally located hotspots (16.7%). These findings suggest that pathologists should focus on peripheral tumor regions when assessing MC in cMCTs and melanomas. Both central and peripheral regions should be considered in CMCs, while a more extensive, comprehensive evaluation may be required in STSs. The observed association between tumor histotype and proliferation pattern likely reflects inherent biological differences among the tumor types studied.

Keywords

Mitotic count, Ki67, image analysis, density map, hotspot.

Introduction

Mitotic count (MC) is one of the most commonly used prognostic factors in veterinary tumor pathology. The association between a high number of mitotic figures (MF) and the aggressive behavior of several neoplasms is widely acknowledged.[1–7]

In veterinary medicine, MC is also included in the histological grading systems of canine mast cell tumors (cMCT),[8,9] mammary carcinomas,[10,11] canine melanomas,[12] and canine soft tissue sarcomas (cSTS).[13,14]

The importance of standardizing histological parameters such as MC, has become increasingly apparent.[15] A major challenge in this standardization lies in the limited reproducibility, primarily due to the lack of clearly defined and reproducible assessment methods.[5,16,17] As a result, the evaluation of several parameters, including MC, often relies on subjective approaches, which hinders consistent comparisons across studies.[18]

Considerable efforts are underway to address these limitations, with proposed guidelines and protocols outlining best practices for measuring specific histological parameters across various tumor types (https://vcgp.org/guidelines-and-protocols/).[18]

In the context of mitotic count (MC) assessment, standardization should address the following key elements:

(1) The histologic morphology of mitotic figures (MF): Only figures from prometaphase to telophase should be counted, focusing on chromosomal aggregates lacking a nuclear membrane;[18]

(2) The size of the counting area: MC should be assessed in a total field area of 2.37 mm^2, which varies depending on the field number (FN) of the ocular and the magnification of the objective lens;[5,17]

(3) The selection of tumor regions for MC assessment: Counting should be performed in areas exhibiting the highest proliferative activity.[19–22]

In many tumor types, the MC is evaluated in regions of maximal mitotic density within tumors.[5,23–26] However, identifying these regions is not straightforward, and there are no clear indications regarding the choice of site with higher proliferative activity across different tumor types.

Some studies suggest that the tumor periphery is the preferred site for mitotic count (MC) assessment, as it often represents the invasive front and may exhibit higher proliferative activity.[5,19] Additionally, tissue fixation is typically more effective at the tumor edges.[5,19,24] A study on human breast carcinoma reported that the tumor periphery contained a higher density of Ki67-positive hotspots, and the proportion of Ki67-positive nuclei in these regions correlated with patient prognosis.[27] However, other studies in human breast carcinoma have found that assessing Ki67 hotspots—regardless of their location within the tumor—yields stronger prognostic value than location-based assessment alone.[22] In veterinary medicine, Bertram and colleagues demonstrated that in canine mast cell tumors (cMCT), the MC varied significantly across different tumor regions. Notably, pathologists were often unable to accurately identify the area with the highest MC when evaluating whole-slide images.[19]

Although MC has long been a mainstay of tumor assessment, until recently, there has been no standardization of any element of this parameter in veterinary pathology. Performing the MC is considered laborious and is characterized by inter-pathologist variation.[28–30]

Standardizing methods should increase reproducibility, decrease subjectivity, and improve the predictability of this commonly used prognostic marker. Automated image

analysis systems represent promising tools for selecting the area with the highest mitotic activity within large tumor sections more accurately.[19]

The aim of this study is to evaluate the spatial distribution of the most proliferative regions in different canine tumor types, in order to identify the most appropriate areas for MC assessment, with the aid of image analysis software.

Methods

Case selection

Tumor types for which the MC is considered a prognostic parameter or is integrated in the grading system were included. Cutaneous canine mast cell tumors (cMCT), canine mammary carcinomas (CMC), oral and cutaneous canine melanomas (malignant melanomas) and canine soft tissue sarcomas (cSTS) were selected from the archives of three institutions. Complex and mixed canine mammary carcinomas were excluded to avoid the confounding effect of myoepithelial or mesenchymal cell proliferation. cSTS cases with a specific diagnosis were enrolled, including perivascular wall tumors, myxosarcomas, fibrosarcomas, liposarcomas, and leiomyosarcomas. cSTS diagnoses were performed by two board certified pathologist experienced in the diagnosis of cSTS and were based on histological features according the most recent classification system[31] and, when necessary, with the application of the appropriate immunohistochemical protocols. Cases with uncertain diagnosis were not included.

Only cases with recognizable tissue orientation and with at least half of a transversal section of the neoplasm available for immunohistochemistry were included. The diagnoses were confirmed by re-assessment of the original hematoxylin and eosin stained sections by two board certified pathologists.

Immunohistochemical labeling

All cases underwent immunohistochemistry for Ki67. Sections 3 to 4 µm thick were obtained from selected paraffin blocks to assess at least half of the transversal section of the neoplasm. Pigmented melanomas underwent de-pigmentation before immunohistochemical staining by incubation for 27 minutes in potassium permanganate (0.25 g/100 mL; Merck, Germany), followed by rinsing in distilled water and immersion for 20/30 seconds – depending on the required level of depigmentation – in oxalic acid (5 g/100 mL; DDK Italia, Italy). Sections were air-dried, dewaxed, and rehydrated. Endogenous peroxidase was blocked by immersion in 3% H_2O_2 in methanol for 30 minutes. Heat-induced antigen retrieval was used (pH 6.0 citrate buffer, in a pressure cooker at 110°C for 20 minutes).

After cooling, sections were preincubated with a blocking solution (10% normal goat serum with phosphate-buffered saline) for 30 minutes. Anti-Ki67 primary antibody (mouse monoclonal, clone MIB-1, dilution 1:1500, Dako, Glostrup, Denmark) was applied and incubated overnight at 4 °C.

Sections were then incubated for 30 minutes at room temperature with anti-mouse biotin-conjugated secondary antibody (dilution 1:200, Dako, Glostrup, Denmark). The reaction was amplified by the avidin-biotin method (ABC kit elite; Vector, Burlingame, CA) and visualized by incubating with 3,30-diaminobenzidine for 2 minutes. Harris' hematoxylin was used as counterstaining. Finally, the sections were dehydrated, and cover-slipped. Sections of the canine small intestine were used as positive control. Negative controls included slides incubated with a nonspecific antibody or the omission of the primary antibody.

Immunohistochemical evaluation and image analysis

The immunohistochemical slides were scanned using Grundium Ocus ® 20 (Tampere, Finland) at 20X magnification (0.25 µm/pixel) to obtain a whole slide image (WSI). The digital images were analysed using the open-source DIA software QuPath v0.5.0.3. Analysis was performed starting with manual selection of the tumor section area (Figure 1A) and positive cell detection tool (Analyze → Cell analysis → Positive cell detection) (Figure 1B). Neoplastic tissue was selected while non-neoplastic tissue adjacent to or entrapped within the neoplasm, necrotic areas, granulation tissue and clearly recognizable inflammatory aggregates were avoided.

Afterward, a density map was created to define areas of higher proliferation and demonstrate their predominant distribution within the section (Figure 1C). For each image, the selection parameters were adjusted iteratively to find the optimal combination, resulting in an accurate selection of Ki67-positive cells (Figure 1D, E).

Each density map was subsequently subjected to visual analysis by experienced pathologists to categorize it into a specific group, classified based on:

- Hotspots distribution: focal/multifocal (one or multiple hot spots were visible) or diffuse (relatively uniform positive cell density within the tumor);
- Hotspot location: central (at the center of the neoplasm), peripheral (at the external regions of the neoplasm), or scattered (when both at central and peripheral regions of the neoplasm).

Examples of the most common spatial arrangements of Ki67 hot spots are depicted in Figure 2. The dataset explores the relationships between two diagnostic variables and the host spots' spatial arrangements. The first diagnostic variable, "Diagnosis 1", identifies broad tumor categories, including CMC, cSTS, melanoma, and cMCT. The second diagnostic variable, "Diagnosis 2," provides a more detailed classification and was applied to soft tissue sarcomas (including perivascular wall tumors,

myxosarcomas, fibrosarcomas, liposarcomas, and leiomyosarcomas) and melanomas (oral or cutaneous).

The analysis was performed using the chi-square test to assess the association between distribution and location (alone and in combination) with diagnosis 1 and diagnosis 2 (when available). This test was chosen to compare the observed frequencies with the expected ones under the null hypothesis, determining statistical significance. A Kruskal-Wallis 1-way analysis of variance was used to assess the association of distribution and location of hot spots with MC, and Ki67 labelling index (expressed as number of positive cells/mm^2). Post-hoc pairwise analysis was performed with Dwass-Steel-Critchlow-Fligner test. Results were considered significant for p-values < 0.05. Statistical analyses were performed using Jamovi (version 2.4.12.0).

Results

A total of 202 cases were collected: 43 melanomas (22 oral and 21 cutaneous), 30 cMCT (21 low grade and 9 high grade), 42 CMC (14 grade 1, 20 grade 2, and 8 grade 3), and 87 STS (49 grade 1, 32 grade 2 and 9 grade 3). STS included 22 perivascular wall tumors, 15 myxosarcomas, 16 leiomyosarcomas, 22 liposarcomas, and 12 fibrosarcomas.

Hot spot distribution was diffuse in 10 cases (5%), focal in 5 (2.5%), and multifocal in 187 (92.6%), and was associated with diagnosis 1 (chi-square = 25.5; $p<0.001$).

Specifically, distribution was diffuse in 2/30 (6.7%) cMCT, 5/42 (11.9%) CMC, 2/43 (4.7%) melanomas and 1/87 (1.1%) cSTS; focal in 4/30 (13.3%) cMCT, 1/42 (2.4%) CMC, 0/43 melanomas and 0/87 cSTS; and multifocal in 24/30 (80%) cMCT, 36/42 (85.7%) CMC, 41/43 (95.3%) melanomas and 86/87 (98.9%) cSTS (Figure 3A).

The hot spot location was central in 12 cases (5.9%), peripheral in 111 (55%), and scattered in 79 (39.1%), and was associated with diagnosis 1 (chi-square = 41.9; $p<0.001$).

Specifically, the location was central in 2/30 (6.7%) cMCT, 7/42 (16.7%) CMC, 0/43 melanomas, and 3/87 cSTS; peripheral in 22/30 (73.3%) cMCT, 25/42 (59.5%) CMC, 33/43 (76.7%) melanomas and 31/87 (35.6%) cSTS; and scattered in 6/30 (20%) cMCT, 10/42 (23.8%) CMC, 10/43 (23.3%) melanomas and 53/87 (60.9%) cSTS (Figure 3B).

Considering the hot spot patterns derived from the combination of distribution and location, the peripheral-multifocal pattern was found in 100/202 cases (49.5%), scattered-multifocal in 79/202 (39.1%), central-multifocal in 8/202 (4.0%), peripheral-diffuse in 6/202 (3.0%), peripheral-focal in 5/202 (2.5%), and central diffuse in 4/202 (2.0%), correlating with diagnosis 1 (chi-square test, $p<0.001$).

Specifically, in cMCT the pattern was peripheral multifocal in 17/30 (56.7%), scattered multifocal in 6/30 (20.0%), peripheral focal in 4/30 (13.3%), central diffuse in 1/30 (3.3%), central multifocal in 1/30 (3.3%), and peripheral diffuse in 1/30 (3.3%).

In CMC, it was peripheral multifocal in 21/42 (50.0%), scattered multifocal in 10/42 (23.8%), central multifocal in 5/42 (11.9%), peripheral diffuse in 3/42 (7.1%), central diffuse in 2/42 (4.8%), and peripheral focal in 1/42 (2.4%).

In melanomas, the patterns were peripheral multifocal in 31/43 (72.1%), scattered multifocal in 10/43 (23.3%), peripheral diffuse in 2/43 (4.7%), and no cases were recorded for the other patterns.

In STS, the pattern was as follows: scattered multifocal in 53/87 (60.9%), peripheral multifocal in 31/87 (35.6%), central multifocal in 2/87 (2.3%), central diffuse in 1/87 (1.1%), and no cases were observed for the remaining patterns.

No statically significant association of the host spot distribution, location and combined pattern with diagnosis 2 (STS histotype and cutaneous versus oral melanoma) was found.

In 10 out of 21 cases of cutaneous melanoma and 13 out of 22 cases of oral melanoma, we were able to assign a third pattern based on the superficial or deep localization of the hotspots. It was visually observed that, in 7 out of 10 (70%) cutaneous melanomas, the hotspots were located on the superficial side, while in 8 out of 13 (62%) cases of oral melanomas, the hotspots were found on the deep side of the neoplasm. Similarly, in 10 MCTs cases, 5 had superficial hotspots, and 5 had deep hotspots.

Finally, in CMC, the localization of the third pattern was assigned in 10 cases, and in 4 of these the distribution mirrored the lobular arrangement of the carcinoma. Detailed results of distribution, localization, Ki67 labeling index, MC, grade and area assessed are reported in Supplementary table 1.

A statistically significant association was found between Ki67 labeling index and both location and distribution, being higher in case with scattered location compared with peripheral ($W=3.33$, $p=0.49$), and in cases with multifocal distribution compared with a diffuse one ($W=4.66$, $p=0.003$).

Discussion

MC is one of the most commonly used histological prognostic factors in veterinary tumor pathology.[5] However, the current method of MC assessment presents significant limitations due to intra-tumoral variability and observer subjectivity. Considerable efforts have been dedicated to overcoming these limitations, resulting in the establishment of a standard area for MC and the morphology of mitotic figures. Nevertheless, there are no guidelines on selecting the tumor region where the count

should be performed.[5] These limitations compromise the reliability of MC as a prognostic factor.

The introduction of computer-assisted diagnosis systems offers promising solutions to address the current challenges of MC.[32] Nevertheless, until most laboratories have entirely switched to digital microscopy,[32] this approach will not be widely applied. Furthermore, a limited number of prognostic studies on canine tumors have used digital microscopy and associated the digital counts with outcome.[21,33]

This study aimed to investigate the regional distribution of proliferative hotspots for different canine tumor types, providing guidelines for pathologists when assessing the MC, following the general rule that MC should be evaluated in areas of highest proliferation.[1]

The multifocal distribution was the predominant location of hot spots for all tumor types included in the study. In STS and melanoma, multifocality was observed in all cases except for one and two cases, respectively. In contrast, a diffuse or focal distribution was found in more than 10% of CMC and cMCT cases, respectively.

We interpreted the multifocality as a consequence of tumor heterogeneity, further confirming the need for more clearly defined indications for selecting the tumor region for MC assessment. This heterogeneity, together with other factors, may be at the root of the low inter-pathologist agreement on MC results. The significant number of CMC with a diffuse distribution may indicate a lower heterogeneity of this tumor type, which may derive from the inclusion of simple carcinoma only.

Regarding the hot spot location, the peripheral one was the most common in all tumor types examined, except for STS. In the past, it has been postulated that the peripheral portion of the tumor, representing the invasive front, was the most proliferative.[34–36] This appears to be especially true in cMCT and canine melanoma, in which the

peripheral distribution represented approximately 75% of the cases. This suggests that, in these tumor types, pathologists should focus mainly at the periphery, when assessing the MC.

Interestingly, despite the higher frequency of the peripheral pattern, CMC included a large number of cases characterized by central hotspots. This result may indicate that, when a low MC is found, or when mitotic figures are difficult to find at the periphery of a CMC, it could be useful to assess the tumor center. Anyway, this indication cannot be extrapolated to all CMC types, as only simple carcinomas were included in this study. Furthermore, the central proliferation in CMC could represent a biologically distinct variant.

On the other hand, in cSTS Ki67 scattered distribution was the most frequent, followed by the peripheral one, in both cases associated with a multifocal distribution. This data indicates a high intra-tumoral heterogeneity of proliferative activity of cSTS cells and suggests that sections should be carefully scrutinized for the detection of regions with high mitotic activity.[31]

Furthermore, the different spatial distribution of Ki67 hotspots may also partially reflect tumor biology. In melanomas and cMCT, proliferative activity is concentrated at the tumor edges, suggesting these areas are the most representative of accurate mitotic diagnosis. Peripheral proliferation in these tumors can be indicative of active margins, which may contribute to greater infiltrative potential. In cSTS, the predominant scattered proliferation could reflect a less focused distribution, potentially associated with their less aggressive tumor behavior. This hypothesis should be confirmed by assessing the spatial distribution of hotspots in a caseload with available clinical follow-ups.

Furthermore, the Ki67 labeling index was significantly higher in cases with a multifocal distribution compared with those with a diffuse pattern, and to a lesser extent, in cases with a scattered location compared with a peripheral one. This may suggest that while a baseline proliferative activity is uniformly present throughout the tumor, peaks of proliferative activity occur in areas where more aggressive neoplastic cell clones undergo selection.

Finally, in some cases, a low correspondence was observed between MC and the Ki67 labeling index. A low MC in tumors with a high Ki67 index is likely due to the count being performed in an area that did not correspond to the most proliferative region. Conversely, a high MC in tumors with a low Ki67 index may result from the count being carried out in a localized hotspot within a tumor otherwise characterized by few proliferative foci and an overall low proliferation rate, considering that the Ki67 index was calculated across the entire section. Both scenarios highlight the need for more detailed guidelines to standardize the selection of tumor regions for MC assessment.

One limitation of this study is the use of an anti-Ki67 antibody, which detects cells at any phase of the cell cycle except for G0, thus labeling not only cells in mitosis but also those in G1, G2, and S phase.[37] As a consequence, it is likely that there is no exact correspondence between Ki67 hotspots and mitotic figures hotspots. Nevertheless, we chose to use this marker since these results can also be applied to the selection of regions for assessing the Ki67 labeling index. This additional prognostic parameter is often required by oncologists for canine melanoma and cMCT, necessitating the identification of highly proliferative regions.[38,39] A second limitation is the exclusion of complex and mixed mammary tumors. This was opted because the separation of the myoepithelial and non-epithelial components would have required a different and more complex image analysis protocol. Finally, we selected cases having

a small diameter, so we could examine at least half of a transversal section. This criterion might have introduced a bias related to a possible different distribution of proliferative hotspots in larger lesions.

Further studies are advisable to confirm our results, to expand the caseload to other tumor types, including subcutaneous cMCT and other mammary tumor types, and to compare the distribution patterns with the biological behavior of the tumors.

In conclusion, the peripheral proliferation observed in melanomas and cMCT, as well as the scattered pattern typical of cSTS, represent distinctive features that may assist in selecting hotspots and could have significant diagnostic and prognostic implications. The association between histological diagnosis and the pattern of proliferation found in this study likely reflects the biological differences among the tumor types studied. A better understanding of proliferative hotspot distribution can contribute to a more targeted prognostic stratification in canine tumors.

1. Avallone G, Rasotto R, Chambers JK, et al. Review of Histological Grading Systems in Veterinary Medicine. *Vet Pathol*. 2021;58(5):809-828.

2. Romansik EM, Reilly CM, Kass PH, Moore PF, London CA. Mitotic Index Is Predictive for Survival for Canine Cutaneous Mast Cell Tumors. *Vet Pathol*. 2007;44(3):335-341.

3. Elston LB, Sueiro FAR, Cavalcanti JN, Metze K. The importance of the mitotic index as a prognostic factor for survival of canine cutaneous mast cell tumors: a validation study. *Vet Pathol*. 2009;46(2):362-364.

4. Horta RS, Lavalle GE, Monteiro LN, Souza MCC, Cassali GD, Araújo RB. Assessment of Canine Mast Cell Tumor Mortality Risk Based on Clinical, Histologic, Immunohistochemical, and Molecular Features. *Vet Pathol*. 2018;55(2):212-223.

5. Meuten DJ, Moore FM, George JW. Mitotic Count and the Field of View Area: Time to Standardize. *Vet Pathol*. 2016;53(1):7-9.

6. Schott CR, Tatiersky LJ, Foster RA, Wood GA. Histologic Grade Does Not Predict Outcome in Dogs with Appendicular Osteosarcoma Receiving the Standard of Care. *Vet Pathol*. 2018;55(2):202-211.

7. Vascellari M, Giantin M, Capello K, et al. Expression of Ki67, BCL-2, and COX-2 in canine cutaneous mast cell tumors: association with grading and prognosis. *Vet Pathol*. 2013;50(1):110-121.

8. Kiupel M, Webster JD, Bailey KL, et al. Proposal of a 2-tier histologic grading system for canine cutaneous mast cell tumors to more accurately predict biological behavior. *Vet Pathol*. 2011;48(1):147-155.

9. Patnaik AK, Ehler WJ, MacEwen EG. Canine cutaneous mast cell tumor: morphologic grading and survival time in 83 dogs. *Vet Pathol*. 1984;21(5):469-474.

10. Mills SW, Musil KM, Davies JL, et al. Prognostic value of histologic grading for feline mammary carcinoma: a retrospective survival analysis. *Vet Pathol*. 2015;52(2):238-249.

11. Peña L, De Andrés PJ, Clemente M, Cuesta P, Pérez-Alenza MD. Prognostic value of histological grading in noninflammatory canine mammary carcinomas in a prospective study with two-year follow-up: relationship with clinical and histological characteristics. *Vet Pathol*. 2013;50(1):94-105.

12. Spangler WL, Kass PH. The histologic and epidemiologic bases for prognostic considerations in canine melanocytic neoplasia. *Vet Pathol*. 2006;43(2):136-149.

13. Kuntz CA, Dernell WS, Powers BE, Devitt C, Straw RC, Withrow SJ. Prognostic factors for surgical treatment of soft-tissue sarcomas in dogs: 75 cases (1986-1996). *J Am Vet Med Assoc*. 1997;211(9):1147-1151.

14. McSporran KD. Histologic grade predicts recurrence for marginally excised canine subcutaneous soft tissue sarcomas. *Vet Pathol*. 2009;46(5):928-933.

15. Meuten D, Munday JS, Hauck M. Time to Standardize? Time to Validate? *Vet Pathol*. 2018;55(2):195-199.

16. Bonert M, Tate AJ. Mitotic counts in breast cancer should be standardized with a uniform sample area. *Biomed Eng Online*. 2017;16(1):28.

17. Ellis PS, Whitehead R. Mitosis counting--a need for reappraisal. *Hum Pathol*. 1981;12(1):3-4.

18. Meuten DJ, Moore FM, Donovan TA, et al. International Guidelines for Veterinary Tumor Pathology: A Call to Action. *Vet Pathol*. 2021;58(5):766-794.

19. Bertram CA, Aubreville M, Gurtner C, et al. Computerized Calculation of Mitotic Count Distribution in Canine Cutaneous Mast Cell Tumor Sections: Mitotic Count Is Area Dependent. *Vet Pathol*. 2020;57(2):214-226.

20. van Diest PJ, Baak JP, Matze-Cok P, et al. Reproducibility of mitosis counting in 2,469 breast cancer specimens: results from the Multicenter Morphometric Mammary Carcinoma Project. *Hum Pathol*. 1992;23(6):603-607.

21. Wei BR, Halsey CH, Hoover SB, et al. Agreement in Histological Assessment of Mitotic Activity Between Microscopy and Digital Whole Slide Images Informs Conversion for Clinical Diagnosis. *Acad Pathol*. 2019;6:2374289519859841.

22. Stålhammar G, Robertson S, Wedlund L, et al. Digital image analysis of Ki67 in hot spots is superior to both manual Ki67 and mitotic counts in breast cancer. *Histopathology*. 2018;72(6):974-989.

401 23. Al-Janabi S, van Slooten HJ, Visser M, van der Ploeg T, van Diest PJ,
402 Jiwa M. Evaluation of mitotic activity index in breast cancer using whole
403 slide digital images. *PLoS One*. 2013;8(12):e82576.

404 24. Baak JPA, Gudlaugsson E, Skaland I, et al. Proliferation is the strongest
405 prognosticator in node-negative breast cancer: significance, error
406 sources, alternatives and comparison with molecular prognostic markers.
407 *Breast Cancer Res Treat*. 2009;115(2):241-254.

408 25. Meyer JS, Cosatto E, Graf HP. Mitotic index of invasive breast carcinoma.
409 Achieving clinically meaningful precision and evaluating tertial cutoffs.
410 *Arch Pathol Lab Med*. 2009;133(11):1826-1833.

411 26. Veta M, van Diest PJ, Willems SM, et al. Assessment of algorithms for
412 mitosis detection in breast cancer histopathology images. *Med Image*
413 *Anal*. 2015;20(1):237-248.

414 27. Gudlaugsson E, Skaland I, Janssen EAM, et al. Comparison of the effect
415 of different techniques for measurement of Ki67 proliferation on
416 reproducibility and prognosis prediction accuracy in breast cancer.
417 *Histopathology*. 2012;61(6):1134-1144.

418 28. Bertram CA, Gurtner C, Dettwiler M, et al. Validation of Digital Microscopy
419 Compared With Light Microscopy for the Diagnosis of Canine Cutaneous
420 Tumors. *Vet Pathol*. 2018;55(4):490-500.

421 29. Meyer JS, Alvarez C, Milikowski C, et al. Breast carcinoma malignancy
422 grading by Bloom-Richardson system vs proliferation index:
423 reproducibility of grade and advantages of proliferation index. *Mod Pathol*.
424 2005;18(8):1067-1078.

30. Tsuda H, Akiyama F, Kurosumi M, et al. Evaluation of the interobserver agreement in the number of mitotic figures of breast carcinoma as simulation of quality monitoring in the Japan National Surgical Adjuvant Study of Breast Cancer (NSAS-BC) protocol. *Jpn J Cancer Res*. 2000;91(4):451-457.

31. Roccabianca P, Schulman F, Avallone G, et al. Pathology of Tumors of Domestic Animals. Vol 3. Kiupel M, ed. Chicago: Foundation, C. L. Davis and S. W. Thompson; 2020.

32. Bertram CA, Gurtner C, Dettwiler M, et al. Validation of Digital Microscopy Compared With Light Microscopy for the Diagnosis of Canine Cutaneous Tumors. *Vet Pathol*. 2018;55(4):490-500.

33. Bertram CA, Bartel A, Donovan TA, Kiupel M. Atypical Mitotic Figures Are Prognostically Meaningful for Canine Cutaneous Mast Cell Tumors. *Vet Sci*. 2023;11(1):5.

34. Baak JPA, Gudlaugsson E, Skaland I, et al. Proliferation is the strongest prognosticator in node-negative breast cancer: significance, error sources, alternatives and comparison with molecular prognostic markers. *Breast Cancer Res Treat*. 2009;115(2):241-254.

35. Bertram CA, Aubreville M, Gurtner C, et al. Computerized Calculation of Mitotic Count Distribution in Canine Cutaneous Mast Cell Tumor Sections: Mitotic Count Is Area Dependent. *Vet Pathol*. 2020;57(2):214-226.

36. Meuten DJ, Moore FM, George JW. Mitotic Count and the Field of View Area: Time to Standardize. *Vet Pathol*. 2016;53(1):7-9.

37. Sun X, Kaufman PD. Ki-67: more than a proliferation marker. *Chromosoma*. 2018;127(2):175-186.

38. Freytag JO, Queiroz MR, Govoni VM, et al. Prognostic value of immunohistochemical markers in canine cutaneous mast cell tumours: A systematic review and meta-analysis. *Vet Comp Oncol*. 2021;19(3):529-540.

39. Smedley RC, Sebastian K, Kiupel M. Diagnosis and Prognosis of Canine Melanocytic Neoplasms. *Vet Sci*. 2022;9(4):175.

459 Figures

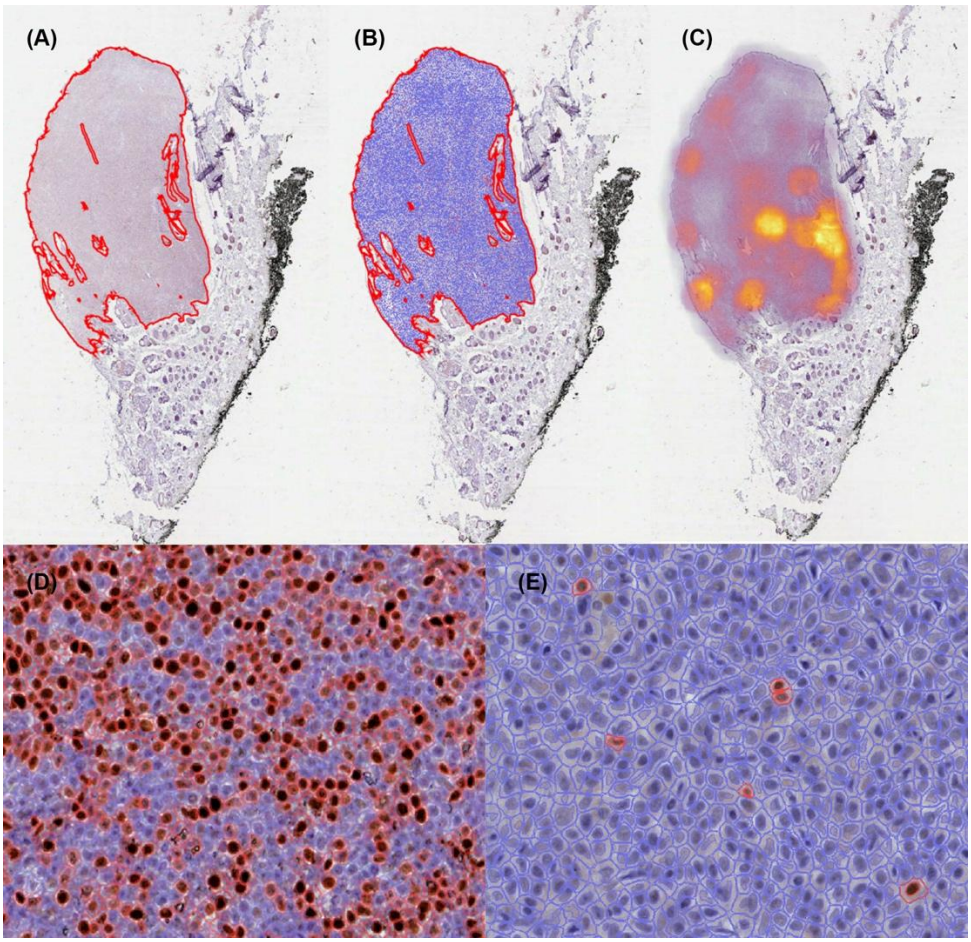

460

461 Figure 1: Examples of image analysis on whole slide image of Ki67
462 immunohistochemistry. A) Selection of the region of interest (ROI) (red line):
463 non-neoplastic tissue, holes and artifacts are excluded; B) Positive cell detection
464 performed on the ROI: in blue are negative cells, in red are positive cells; C)
465 Density maps showing the regions of the tumor with higher positive cell density
466 (yellow shade); D) Positive cell detection in a canine mast cell tumor with high
467 proliferative activity, and E) in a canine soft tissue sarcoma with low proliferative
468 activity. In blue are negative cells, in red are positive cells

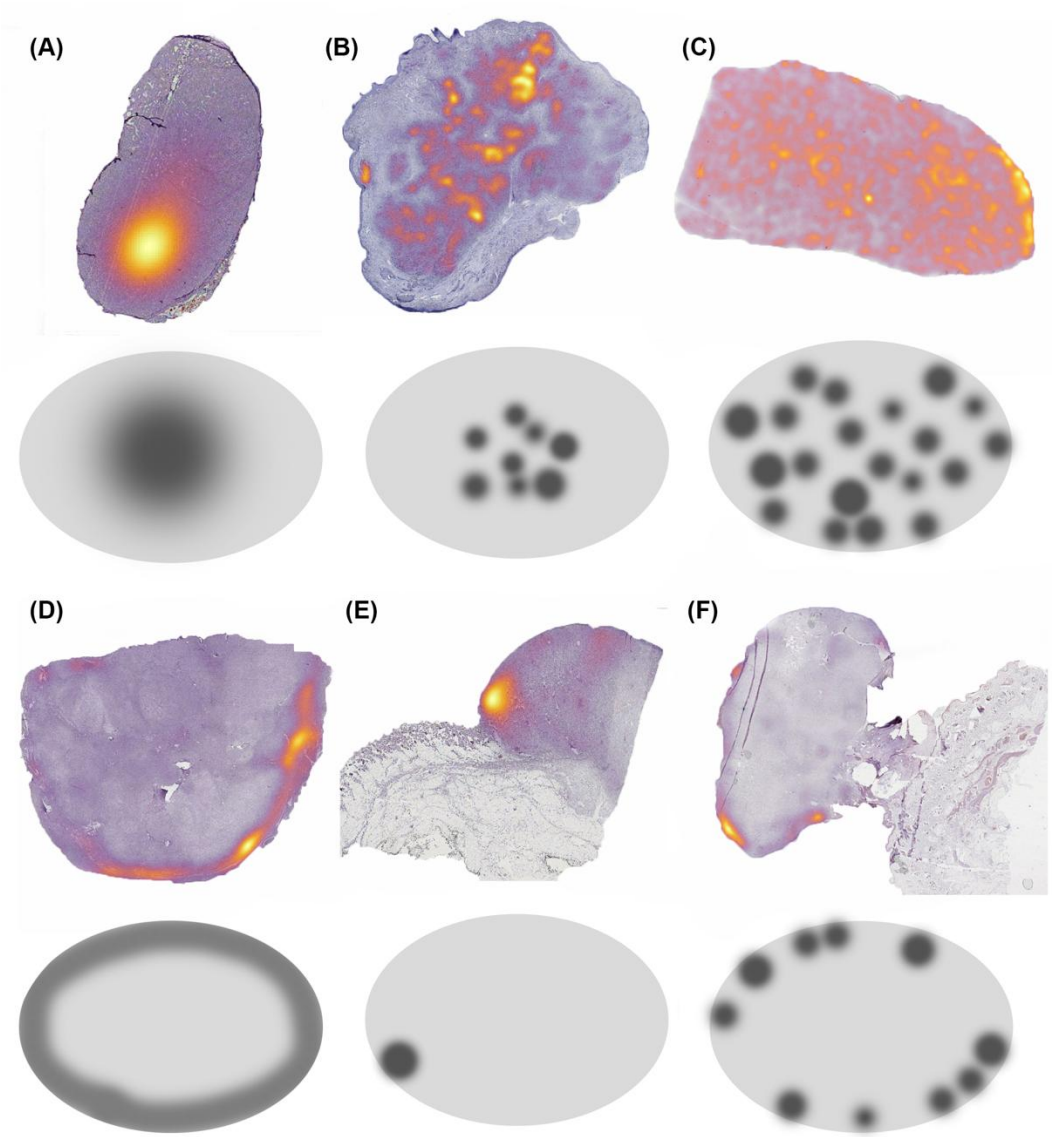

Figure 2: Examples of the most frequent patterns of density maps and corresponding example pictograms. A) Central diffuse pattern in a canine mammary carcinoma; B) Central multifocal pattern in a canine mammary carcinoma; C) Scattered multifocal pattern in a canine liposarcoma; D) Peripheral diffuse pattern in a canine perivascular wall tumor; E) Peripheral focal pattern in a cutaneous mast cell tumor; F) Peripheral multifocal pattern in a canine cutaneous melanoma.

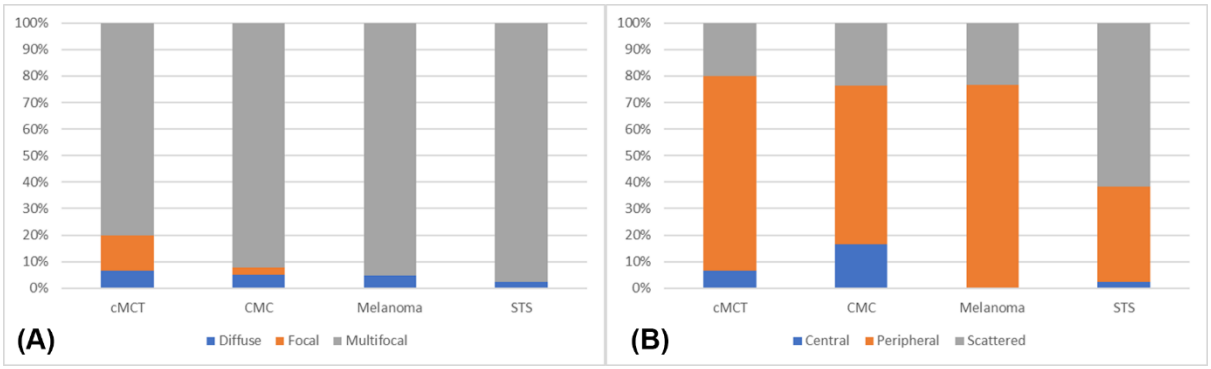

Figure 3: Bar plots depicting the percentage of cases presenting A) diffuse, focal or multifocal distribution and B) central, peripheral and scattered location. Mast cell tumors have a higher percentage of focal distribution and soft tissue sarcomas have a higher percentage of scattered location. cMCT: cutaneous mast cell tumors

CMC: canine mammary carcinoma

STS: soft tissue sarcoma